Endothelial overexpression of *LOX-1* increases plaque formation and promotes atherosclerosis *in vivo*

Alexander Akhmedov[1,2†], Izabela Rozenberg[1,2†], Francesco Paneni[1,2], Giovanni G. Camici[1,2], Yi Shi[1,2], Carola Doerries[1,2], Anna Sledzinska[2,3], Pavani Mocharla[1,2], Alexander Breitenstein[1,2], Christine Lohmann[1,2], Sokrates Stein[1,2], Tobias von Lukowicz[1,2], Michael O. Kurrer[4], Jan Borén[5], Burkhard Becher[2,3], Felix C. Tanner[1,2], Ulf Landmesser[1,2], Christian M. Matter[1,2], and Thomas F. Lüscher[1,2*]

[1]Cardiovascular Research, Institute of Physiology, University of Zurich; and Cardiovascular Center, Cardiology, University Hospital Zurich, 8091 Zurich, Switzerland; [2]Zurich Center of Integrative Human Physiology, University of Zurich, Zurich, Switzerland; [3]Neuroimmunology Unit, Institute of Experimental Immunology, University of Zurich, Zurich, Switzerland; [4]Division of Pathology, University Hospital Zurich, Zurich, Switzerland; and [5]Sahlgrenska Center for Cardiovascular and Metabolic Research, University of Göteborg, Gothenburg, Sweden

This paper was handled by GUEST EDITOR Filippo Crea (Universita Catolica del Santo Cuore; filippo.crea@rm.unicatt.it)

Aims	Lectin-like oxLDL receptor-1 (LOX-1) mediates the uptake of oxidized low-density lipoprotein (oxLDL) in endothelial cells and macrophages. However, the different atherogenic potential of LOX-1-mediated endothelial and macrophage oxLDL uptake remains unclear. The present study was designed to investigate the *in vivo* role of endothelial LOX-1 in atherogenesis.
Methods and results	Endothelial-specific *LOX-1* transgenic mice were generated using the *Tie2* promoter (*LOX-1TG*). Oxidized low-density lipoprotein uptake was enhanced in cultured endothelial cells, but not in macrophages of *LOX-1TG* mice. Six-week-old male *LOX-1TG* and wild-type (WT) mice were fed a high-cholesterol diet (HCD) for 30 weeks. Increased reactive oxygen species production, impaired endothelial nitric oxide synthase activity and endothelial dysfunction were observed in *LOX-1TG* mice as compared with WT littermates. LOX-1 overexpression led to p38 phosphorylation, increased nuclear factor κB activity and subsequent up-regulation of vascular cell adhesion molecule-1, thereby favouring macrophage accumulation and aortic fatty streaks. Consistently, HCD-fed double-mutant *LOX-1TG/ApoE*$^{-/-}$ displayed oxidative stress and vascular inflammation with higher aortic plaques than *ApoE*$^{-/-}$ controls. Finally, bone marrow transplantation experiments showed that endothelial LOX-1 was sufficient for atherosclerosis development *in vivo*.
Conclusions	Endothelial-specific LOX-1 overexpression enhanced aortic oxLDL levels, thereby favouring endothelial dysfunction, vascular inflammation and plaque formation. Thus, LOX-1 may serve as a novel therapeutic target for atherosclerosis.
Keywords	Endothelium • Vascular inflammation • Atherosclerosis

Introduction

Oxidized low-density lipoprotein (oxLDL) is internalized by endothelial cells and macrophages and its accumulation in the subendothelial space is a key event preceding plaque formation.[1,2] Plasma levels of oxLDL are increased in both experimental and human atherosclerosis. While in macrophages, oxLDL is internalized by several receptors such as scavenger receptor A (SR-A), CD36, and CD68,[3] in endothelial cells, its uptake depends solely on LOX-1.[4] LOX-1 is a type II membrane glycoprotein that has a C-terminal extracellular C-type lectin-like domain, which is essential for binding to oxLDL.[5]

[†] These authors contributed equally to this work.

[*] Corresponding author. Tel: +41 44 255 21 21, Fax: +41 44 255 42 51, Email: cardiotfl@gmx.ch

Endothelial dysfunction induced by oxLDL has been implicated in atherogenesis.[6] Moreover, *LOX-1* expression is increased in atherosclerotic plaques and its genetic deletion is associated with reduced plaque formation in hypercholesterolemic mice.[7–9] In endothelial cells, oxLDL-induced activation of LOX-1 triggers the expression of inflammatory genes involved in endothelial dysfunction and atherogenesis such as monocyte chemotactic protein-1 (MCP-1), intercellular adhesion molecule-1 (ICAM-1), and vascular cell adhesion molecule-1 (VCAM-1).[10,11] Moreover, LOX-1 activation *in vitro* reduces nitric oxide (NO) availability via increased reactive oxygen species (ROS) generation.[12] Although these studies provided interesting insights on the putative role of LOX-1 in atherogenesis, the *in vivo* effects of endothelial *LOX-1* activation remain to be elucidated.

To specifically explore the role of LOX-1 in the vascular endothelium, endothelial-specific *LOX-1* transgenic mice were generated using the *Tie2* promoter (*LOX-1TG*). We found that endothelial-specific overexpression of LOX-1 is associated with atherosclerotic features resulting from increased oxidative stress and NFκB-driven inflammation. Our results highlight opportunities for selective inhibition of LOX-1 in conditions of hypercholesterolemia.

Methods

Generation of LOX-1 transgenic mice

To obtain mice overexpressing LOX-1 in endothelial cells, a murine tyrosine kinase receptor *Tie2* promoter was used (*Figure 1*A). Targeted *LOX-1* gene expression in endothelial cells was achieved using the coding sequence for the murine *LOX-1* gene inserted into the expression vector pSP14/15, which contains the murine 2 kb *Tie2* promoter together with 10 kb *Tie2* enhancer originated from intron 1 of the endogenous murine *Tie2* gene (the pSP14/15 vector was a kind gift of Thomas N. Sato, MD, PhD, University of Texas, TX, USA) (see Supplementary material online, Methods).

To obtain *LOX-1/ApoE*$^{-/-}$ double-mutant mice, hemizygous *LOX-1* transgenic mice from the line, carrying maximal number of copies of the transgene, were cross-bred with homozygous ApoE knockout mice on a C57BL/6 background. Offsprings carrying the *LOX-1* transgene and being heterozygous for the *ApoE* locus were used to generate *LOX-1TG/ApoE*$^{-/-}$ mice (see Supplementary material online, Methods). All animal experiments were performed on male mice. All procedures were in accordance with institutional guidelines and approved by the local animal committee.

Bone marrow transplantation

Bone marrow transplantation experiments were performed as described[13] (for details, see Supplementary material online, Methods).

Diet, tissue harvesting and processing

See Supplementary material online, Methods.

Plaque quantifications

Serial cross sections of the aortic root (8 μm thickness) from *LOX-1TG* and corresponding C57BL/6 wild-type (WT) mice were cut and thaw-mounted on glass slides for oil red O staining. For quantification of atherosclerotic plaques in *LOX-1TG/ApoE*$^{-/-}$ and *ApoE*$^{-/-}$ mice, *en face* analysis of thoraco-abdominal aortas was performed as described.[14] Plaque area was visualized by fat staining (oil red O), photographed with a digital camera (Olympus DP70, 12.5 megapixels) that was mounted on

binocular microscope (Olympus Schweiz AG), and quantified (Analysis 5; SoftImaging System).

Plasma lipids

Plasma cholesterol and triglycerides levels were determined using Infinity™ Cholesterol, Infinity™ Triglycerides (Thermo Electron Corporation Standard) and MC Cal (Abbott) (see Supplementary material online, Methods).

Oxidized low-density lipoprotein measurements

To determine mouse oxLDL concentrations in mouse serum and aorta homogenates isolated from 12- to 14-week-old *LOX-1TG* and corresponding WT male mice, commercially available Mouse Oxidized Low Density Lipoprotein ELISA Kit (Cusabio Biotech, Wuhan, PR China) was used according to the manufacturer's instructions.

Endothelium-dependent relaxation of intact aorta

The thoracic aortas of *ApoE*$^{-/-}$ and *LOX-1TG/ApoE*$^{-/-}$ mice were isolated after 20 weeks of HCD. Aortas were dissected, excised and placed into cold modified Krebs−Ringer solution of the following composition (mM): NaCl 118, KCl 4.7, CaCl$_2$ 2.5, MgSO$_4$ 1.2, NaHCO$_3$ 25.0, KH$_2$PO$_4$ 1.18 and calcium disodium EDTA 0.026, glucose 11.1 (control solution). The aortic rings (2 mm in length) were suspended in organ chambers containing control solution (37°C) aerated with 95% O$_2$ and 5% of CO$_2$. They were connected to a force transductor (Powerlab Model ML785 and ML119). Changes in isometric tension were recorded. The rings were stretched progressively to their optimal resting tension (0.75 g) and were allowed to equilibrate for 90 min. Concentration−response curves were obtained in a cumulative way. To study endothelium-dependent relaxations to acetylcholine, the preparations were exposed to U 46619 [in order to obtain 50−70% of response to KCl (60 mM)]. Sodium nitroprusside (SNP) was applied to study endothelium-independent relaxation.

Measurement of total reactive oxygen species production by electron spin resonance spectroscopy

Total levels of ROS were determined in murine descending aorta sections by electron spin resonance (ESR) spectroscopy using the spin probe 1-hydroxy-3-methoxycarbonyl-2,2,5,5-tetramethyl-pyrrolidine and an e-scan ESR spectrometer (Bruker). The intensity of ESR spectra was quantified after calibration of ESR signals with the free radical 3-carboxy-2,2,5,5-tetramethyl-1-pyrrolidinyloxy. The intensity values were divided by the dry weight of aorta sections.

Isolation of murine endothelial cells

Murine aortic endothelial cells were isolated as described[15] (for details, see Supplementary material online, Methods).

Lipid uptake

Endothelial cells or macrophages were stimulated with 10 μg/mL Dil-oxLDL (Intracel).[16,17] After 6 h cells were harvested and stained with anti-mouse CD105 antibody (Pharmingen), followed by incubation with FITC-labelled anti-rat secondary antibody (Molecular Probes). Mean fluorescence was monitored with FACS (BD, Canto II) and analysis of the data was performed using FlowJo software.
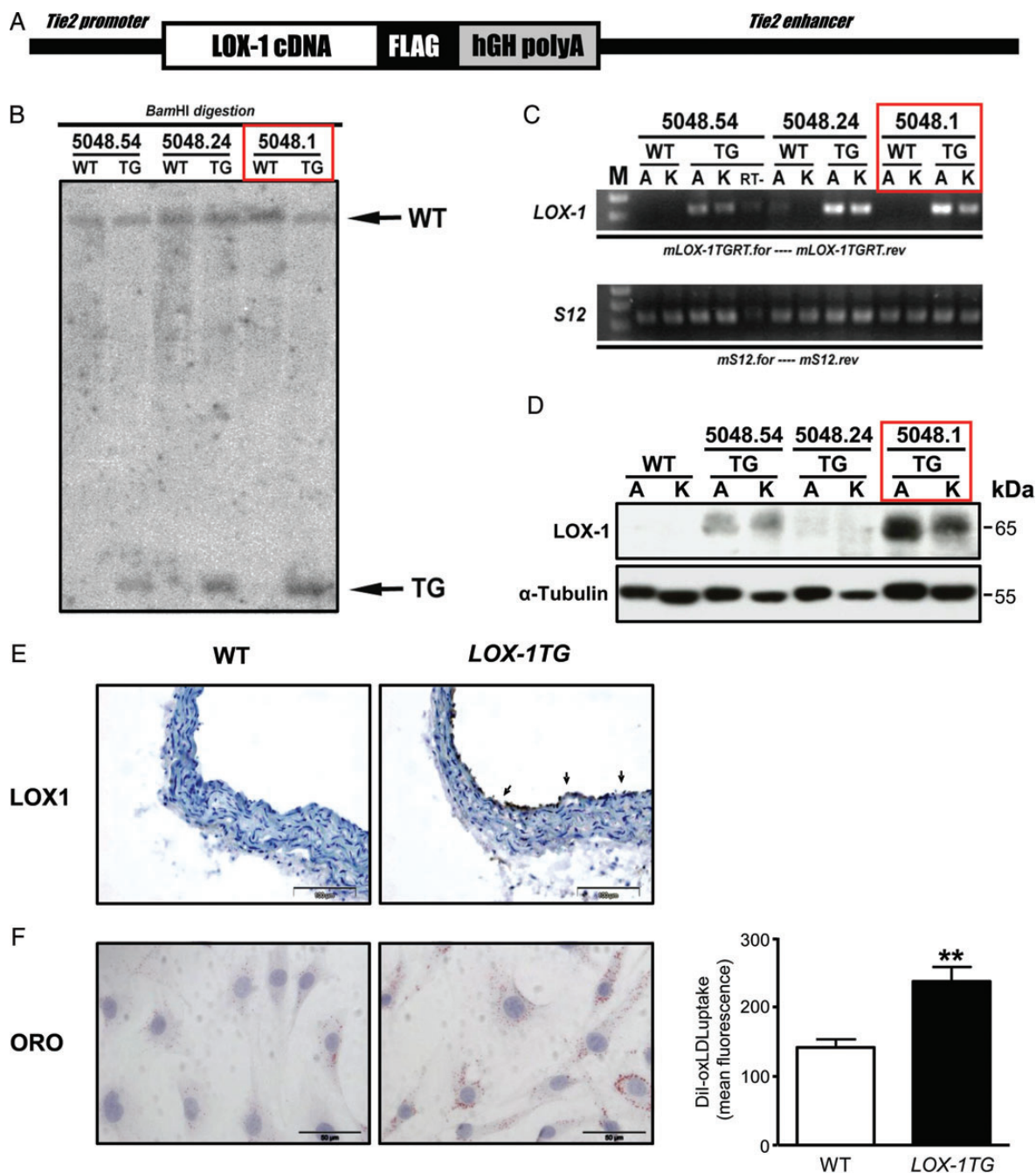
Figure 1 Generation and characterization of endothelial-specific *LOX-1TG* mice. (A) Scheme of endothelial-specific *LOX-1* transgenic construct. (B) Southern blot analysis of F1 generation. Genomic DNA isolated from tail biopsies was digested with *Bam*HI, and hybridized with *LOX-1*-specific radioactively labelled probe. The presence of additional *Bam*HI restriction site located within *LOX-1* cDNA introduced into murine genome upon integration of the transgenic construct allowed to detect the corresponding band in transgenic lanes with the specific probe used. This band is absent in wild-type lanes. (C) real-time polymerase chain reaction analysis. Total RNA isolated from either aorta (A) or kidney (K) of three different transgenic lines 5048.54, 5048.24, and 5048.1 are transformed into cDNA and amplified with *LOX-1*-specific primers. As a loading control, murine *S12*-specific primers are used. Real-time-negative control without reverse transcriptase; *M*, 100 bp DNA molecular weight marker. (D) Western blot of aortic lysates using anti-murine LOX-1 antibody. Anti-murine α-tubulin antibody is used as a loading control. Transgenic line 5048.1 (red rectangle) is used for all subsequent experiments. (E) Aortic cross sections from C57BL/6 wild type (left) and *LOX-1TG* (right) are stained with anti-murine LOX-1 antibody. Bar = 100 μm. (F) Murine endothelial cells isolated from *LOX-1TG* mice and stimulated with DiI-oxidized low-density lipoprotein for 6 h, reveal increased oxidized low-density lipoprotein uptake compared with endothelial cells from wild-type mice as shown by oil red O staining and monitored by FACS with an anti-mouse CD105 antibody. Quantification of FACS measurements is given as mean fluorescence of the CD105-positive cells; *n* = 4 for each group, **P < 0.01.

RT−PCR analysis, immunohistochemistry and western blotting

See Supplementary material online, Methods.

Statistical analysis

Data are presented as mean $\pm$ SEM. Statistical significance was calculated using either ANOVA with *post hoc* Tukey's test or Student's unpaired *t*-test. Significance at the level of two-tailed $P < 0.05$ was accepted for the corresponding statistical analysis.

Results

Generation and molecular characterization of LOX-1 transgenic mice

To obtain mice overexpressing LOX-1 in endothelial cells, a murine tyrosine kinase receptor *Tie2* promoter was used (*Figure 1A*). Mice overexpressing LOX-1 in endothelial cells carried a different copy number of *LOX-1* transgene (*Figure 1B*). The line 5048.1, which showed the highest transgene expression, was selected for further experiments (*Figure 1B* through *D*). LOX-1 expression was the highest in the aorta, while lower expression levels were observed in the kidney (*Figure 1C*). Increased aortic expression of LOX-1 in transgenic mice was confirmed by Western blot (*Figure 1D*). In contrast, LOX-1 was not detectable in WT littermates (*Figure 1D*). Immunohistochemistry confirmed that overexpression of LOX-1 was confined to the vascular endothelium (*Figure 1E*). Moreover, oxLDL uptake was increased only in endothelial cells isolated from *LOX-1TG* but not WT mice (*Figure 1F*). Importantly, in cultured macrophages oxLDL uptake did not differ between *LOX-1TG* and WT mice (Supplementary material online, *Figure S1*). Plasma lipoprotein levels remained unchanged in transgenic mice compared with their WT littermates (*Table 1*). In contrast, vascular oxLDL levels were increased in *LOX-1TG* mice as compared with WT (Supplementary material online, *Table S1*) suggesting a key role of endothelial LOX-1 for oxLDL uptake *in vivo*.

Endothelial LOX-1 overexpression promotes fatty streak formation

To examine the effects of endothelial LOX-1 overexpression on the initial stages of atherogenesis, we fed *LOX-1TG* and WT mice a high-cholesterol diet (HCD) for 30 weeks (*Figure 2A*). In *LOX-1TG* mice, aortic fatty streak formation was significantly increased (*Figure 2B*).

Upon initiation of plaque formation, oxLDL activates inflammatory pathways in vascular cells. In line with this concept, immunohistochemical stainings of aortas showed increased endothelial expression of VCAM-1 in *LOX-1TG* mice compared with WT (*Figure 2C*). Adhesion molecules are important for recruiting inflammatory cells to the activated endothelium. Indeed, the number of activated macrophages, as assessed by the number of CD68-positive cells, was increased in aortas of *LOX-1TG* mice (*Figure 2D*).

Endothelial LOX-1 overexpression on ApoE background increases atherosclerosis

To investigate whether *LOX-1* overexpression plays a role in plaque formation, *LOX-1TG* mice were crossed with apolipoprotein E knockout (*ApoE*$^{-/-}$, C57BL/6 background) mice, a widely used mouse model for studying atherosclerosis.[18] The resulting *LOX-1TG/ApoE*$^{-/-}$ and *ApoE*$^{-/-}$ male littermates were fed a HCD for 20 weeks (*Figure 3A*). Interestingly, *en face* plaque area was almost two-fold increased in *LOX-1TG/ApoE*$^{-/-}$ as compared with *ApoE*$^{-/-}$ littermates (*Figure 3B*). To determine the effects of endothelial-specific LOX-1 overexpression on vascular inflammation, immunohistochemical staining for VCAM-1 and P-selectin was performed on cross sections of aortic roots. Morphometric analyses revealed increased expression levels of VCAM-1 and P-selectin in *LOX-1TG/ApoE*$^{-/-}$ (*Figure 3C* and Supplementary material online, *Figure S2*). mRNA analysis for VCAM-1 confirmed these results (data not shown). In addition, the number of plaque macrophages (CD68-positive area; *Figure 3D*) and T-cells (CD3-positive area; *Figure 3E*) was increased in *LOX-1-1TG/ApoE*$^{-/-}$ mice.

To understand whether endothelial LOX-1 is required for atherosclerosis development *in vivo*, bone marrow transplantation experiments were performed. Bone marrow cells isolated from *ApoE*$^{-/-}$ or *LOX-1-1TG/ApoE*$^{-/-}$ donor mice were transplanted into irradiated 5-week-old recipient *ApoE*$^{-/-}$ and *LOX-1-1TG/ApoE*$^{-/-}$ mice (Supplementary material online, *Figure S3A*). Chimeric *LOX-1-1TG/ApoE*$^{-/-}$ recipient mice receiving either *ApoE*$^{-/-}$ or *LOX-1-1TG/ApoE*$^{-/-}$ bone marrow cells still showed more atherosclerotic plaques than those recipient *ApoE*$^{-/-}$ mice receiving either bone marrow (Supplementary material online, *Figure S3B*). In addition, immunostaining of aortic cross section from *ApoE*$^{-/-}$ and *LOX-1-1TG/ApoE*$^{-/-}$ mice kept 20 weeks on HCD with LOX-1 and CD68 showed no LOX-1 expression in activated macrophages (Supplementary material online, *Figure S3C*). Finally, FACS analysis of blood and spleen samples from transplanted mice revealed no difference in frequencies of monocytes, T-cell subtypes or macrophages (Supplementary material online, *Figure S4*).

Table I Plasma lipid profiles in wild-type, *LOX-1TG*, *ApoE*$^{-/-}$, and *LOX-1TG/ApoE*$^{-/-}$ mice

	WT (*n* = 5)	**LOX-1TG** (*n* = 6)	**ApoE**$^{-/-}$ (*n* = 8)	**LOX-1TG/ApoE**$^{-/-}$ (*n* = 10)
Total cholesterol (mmol/L)	5.64 $\pm$ 1.20	6.27 $\pm$ 0.94	19.97 $\pm$ 2.98**	16.98 $\pm$ 2.83**
Triglycerides (mmol/L)	0.77 $\pm$ 0.07	0.75 $\pm$ 0.03	0.84 $\pm$ 0.18	1.13 $\pm$ 0.28
Free fatty acids (mmol/L)	0.30 $\pm$ 0.06	0.28 $\pm$ 0.08	0.36 $\pm$ 0.06	0.44 $\pm$ 0.07

Statistical significance was calculated using analysis of variance. **$P < 0.005$ compared with wild-type and *LOX-1TG*, mean $\pm$ SEM.
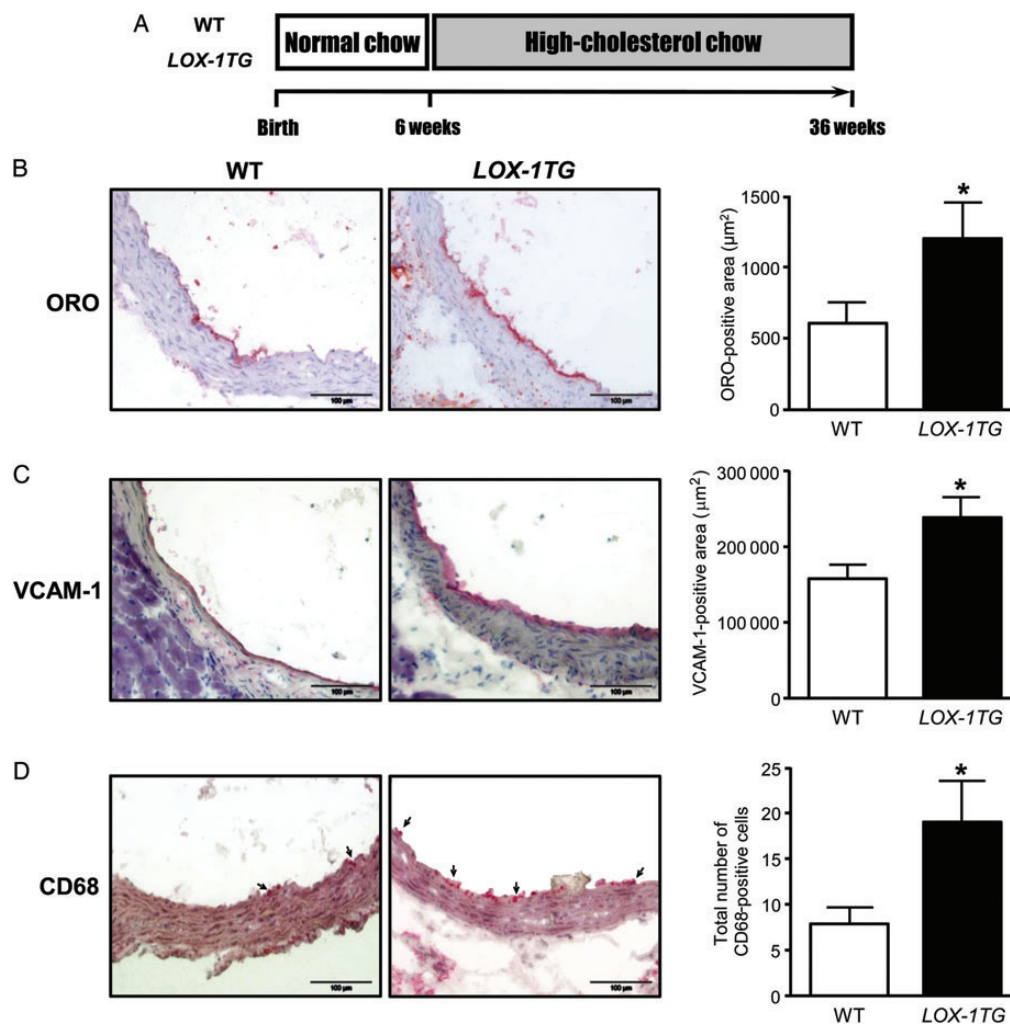
Figure 2 Increased aortic fatty streak formation, expression of VCAM-1, and CD68 in *LOX-1TG* mice. (*A*) Scheme of the diet set up. Six-week-old male *LOX-1TG* and wild-type control mice kept on normal chow diet were then fed a high-cholesterol diet for additional 30 weeks. (*B*) Immunostaining of aortic roots from *LOX-1TG* mice 30 weeks after high-cholesterol diet showed increased lipid accumulation as assessed by oil red O staining with corresponding quantification. Immunohistochemistry of aortic roots from *LOX-1TG* mice for (*C*) VCAM-1 and (*D*) CD68 showed increased inflammation compared with wild-type mice; $n = 10$ for wild-type and $n = 8$ for *LOX-1TG*, *$P < 0.05$. Values are expressed as mean $\pm$ SEM. Bar $= 100$ μm.

LOX-1 overexpression increases reactive oxygen species production and inflammation

As endothelial dysfunction precedes plaque formation, we assessed endothelium-dependent vasorelaxation to acetylcholine in isolated aortic rings obtained from WT, *LOX-1TG*, *ApoE*$^{-/-}$ and *LOX-1TG/ApoE*$^{-/-}$ mice. Whereas no difference was seen in endothelium-dependent vasorelaxation to acetylcholine between *LOX-1TG* and WT mice, in *LOX-1TG/ApoE*$^{-/-}$ mice, acetylcholine-induced endothelium-dependent vasorelaxation was impaired (pEC50 ($-$log M): 6.34 ± 0.12); $E_{\max}$ (% of contraction) $6.52 \pm 3.05\%$ compared with that of *ApoE*$^{-/-}$ mice (6.67 ± 0.40, $P < 0.05$; $E_{\max}$ (% of contraction) $22.18 \pm 6.68\%$, $P < 0.05$) (*Figures 4A* and *5A*, respectively). In contrast, endothelium-independent relaxation to SNP was similar

(data not shown). Next, we tested whether impaired endothelial function would have any impact on endothelial nitric oxide synthase (eNOS) activity. Indeed, eNOS activation through phosphorylation was markedly reduced in both *LOX-1TG* and *LOX-1TG/ApoE*$^{-/-}$ mice (*Figures 4B* and *5B*, respectively; Supplementary material online, *Figure S5A*). Since eNOS is known to be redox sensitive and thus can be regulated by ROS, we measured ROS in aortas isolated from *LOX-1TG* and *LOX-1TG/ApoE*$^{-/-}$. Aortic levels of ROS in both transgenic groups were markedly increased compared with corresponding littermate controls, but they decreased when aortas from both *LOX-1TG* and *LOX-1TG/ApoE*$^{-/-}$ were pre-incubated with superoxide dismutase, a known scavenger of superoxide (*Figures 4C* and *5C*, respectively).

LOX-1 receptor activation leads to accumulation of ROS and in turn activates a cascade of redox-sensitive events including MAPK
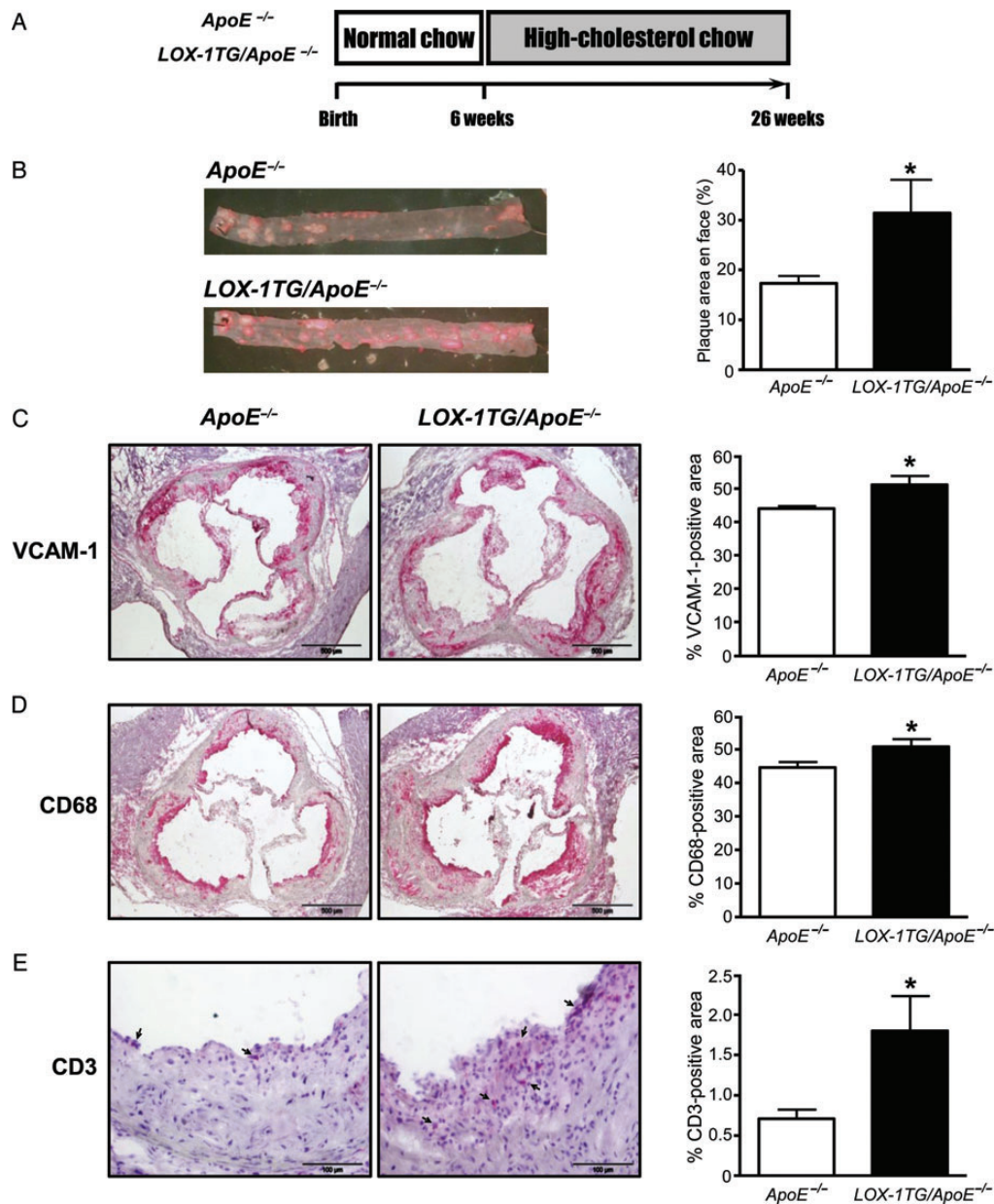
Figure 3 Increased aortic plaque formation and inflammation in *LOX-1TG/ApoE*$^{-/-}$ mice. (A) Twenty-six-week-old mice were sacrificed for tissue isolation. Six-week-old male *LOX-1TG/ApoE*$^{-/-}$ and *ApoE*$^{-/-}$ mice kept on normal chow diet were fed a high-cholesterol diet for 20 weeks (lower panel). Twenty-six-week-old mice were euthanized for tissue harvesting. (B) *En face* plaque staining with corresponding quantification of thoraco-abdominal aortas from *LOX-1TG/ApoE*$^{-/-}$ mice after 20 weeks of high-cholesterol diet showed increased lipid accumulation; $n = 12$ for *ApoE*$^{-/-}$ and $n = 9$ for *LOX-1TG/ApoE*$^{-/-}$, *$P < 0.05$. (C) Immunostaining of aortic roots from *LOX-1TG/ApoE*$^{-/-}$ and *ApoE*$^{-/-}$ mice with VCAM-1 antibody with corresponding quantification; $n = 7$; *$P < 0.05$. (D, E) Cross sections of aortic roots from *LOX-1TG/ApoE*$^{-/-}$ mice stained with (D) antibody against CD68, or (E) antibody against CD3 (arrows indicate positive staining) showed increased macrophage and T cell accumulation compared with *ApoE*$^{-/-}$ mice; $n = 7$ for each group, *$P < 0.05$. Bar = 500 μm (C, D) and 100 μm (E). Values are expressed as mean ± SEM. Statistical significance was calculated using unpaired Student's *t*-test.

pathways.[12,19–22] To test this in our setting, both protein expression and phosphorylation of p38 MAPK were assessed in *LOX-1TG* aortic lysates and were both increased compared with non-transgenic controls (*Figure 4D* and Supplementary material online, *Figure S5B*). Further, activation of the redox-sensitive transcription factor nuclear factor κB (NFκB) was increased in *LOX-1TG* mice due to increased binding of the p65 subunit of NFκB to DNA (*Figure 4E*). Finally, we assessed the expression of *VCAM-1* and *E-selectin*, both known to be regulated by ROS through NFκB.[23] Indeed, mRNA expression of *VCAM-1* and *E-selectin* was higher in aortic lysates obtained from transgenic mice (*Figure 4F* and Supplementary material online, *Figure S5C*).
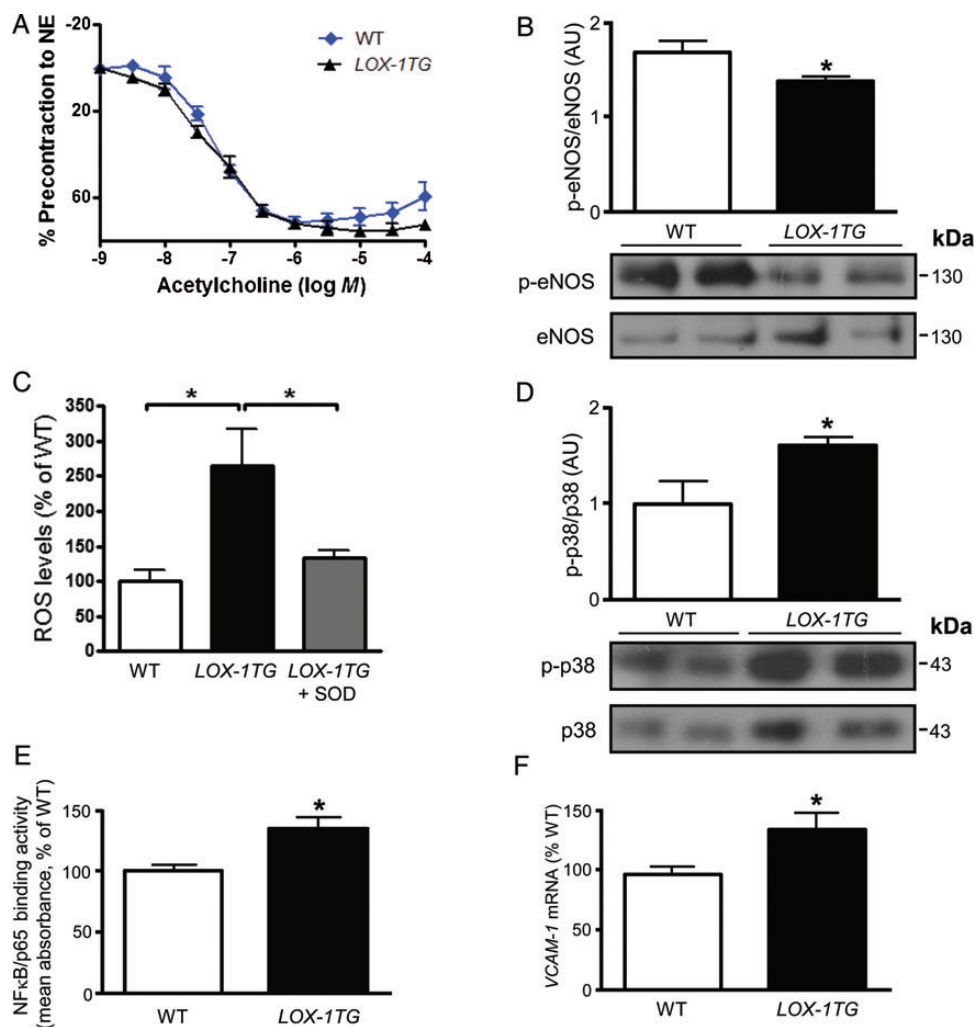
Figure 4 Increased fatty streaks are associated with decreased endothelial nitric oxide synthase phosphorylation, increased ROS levels, p38 phosphorylation and NFκB activation in *LOX-1TG* mice. (A) Relaxation to acetylcholine in aortic rings from WT (blue line) and *LOX-1TG* (black line). Values were normalized to preconstruction with U46619 and shown as mean $\pm$ SEM. $n = 6$ per genotype. (B) Western blot reveals decreased endothelial nitric oxide synthase activation through phosphorylation of Ser1177 residue in aortic lysates from *LOX-1TG* mice. Quantification of protein expression is given as ratio to total endothelial nitric oxide synthase expression levels; $n = 4$ for each group, *$P < 0.05$. Statistical significance was calculated with unpaired Student's *t*-test. (C) Measurements of total ROS production by ESR spectroscopy in aortas show increased ROS levels in *LOX-1TG* mice compared with WT controls. Pre-treatment of aortas from *LOX-1TG* mice with 150 U/mL superoxide dismutase (SOD) significantly reduces ROS accumulation. Quantification is given as a percentage of average control value; $n = 6$ for each group, *$P < 0.05$. (D) Western blot shows increased p38 phosphorylation in aortic lysates from *LOX-1TG* mice. Quantification of protein expression is given as ratio to total p38 expression levels; $n = 4$ for each group, *$P < 0.05$. (E) Increased p38 phosphorylation is further associated with increased nuclear translocation and binding capacity of NFκB as shown by DNA-binding assay for RelA/p65 subunit of NFκB in aortic lysates. Quantification of binding activity is given as mean absorbance and normalized to the average value of unstimulated *LOX-1TG* endothelial cells; $n = 6$ for each group, *$P < 0.05$. (F) Increased NFκB further activates expression of inflammation molecule VCAM-1. The *VCAM-1* mRNA was analysed by quantitative real time PCR. RNA was normalized to the internal control *S12* ($n = 6$ in each group). Data are shown as percentage of WT average. Values are expressed as the mean $\pm$ standard error of mean (SEM). *$P < 0.05$ vs. control wild-type (WT) mice.

Discussion

In the present study, we sought to elucidate whether and through which mechanisms endothelial LOX-1 accelerates fatty streak formation and atherosclerosis development. To this end, we generated *Tie2-LOX-1TG* mice with endothelium-targeted LOX-1 overexpression and compared the development of atherosclerosis in these mice and their WT littermates. Our results suggest that endothelial LOX-1 is critically involved in the development of endothelial dysfunction, vascular inflammation and atherosclerotic lesions. Several lines of evidence support our conclusions: (i) endothelial-specific LOX-1 overexpression accelerates fatty streak formation, induces adhesion molecule expression, and increases macrophage recruitment; (ii) LOX-1 overexpression in $ApoE^{-/-}$ mice causes endothelial
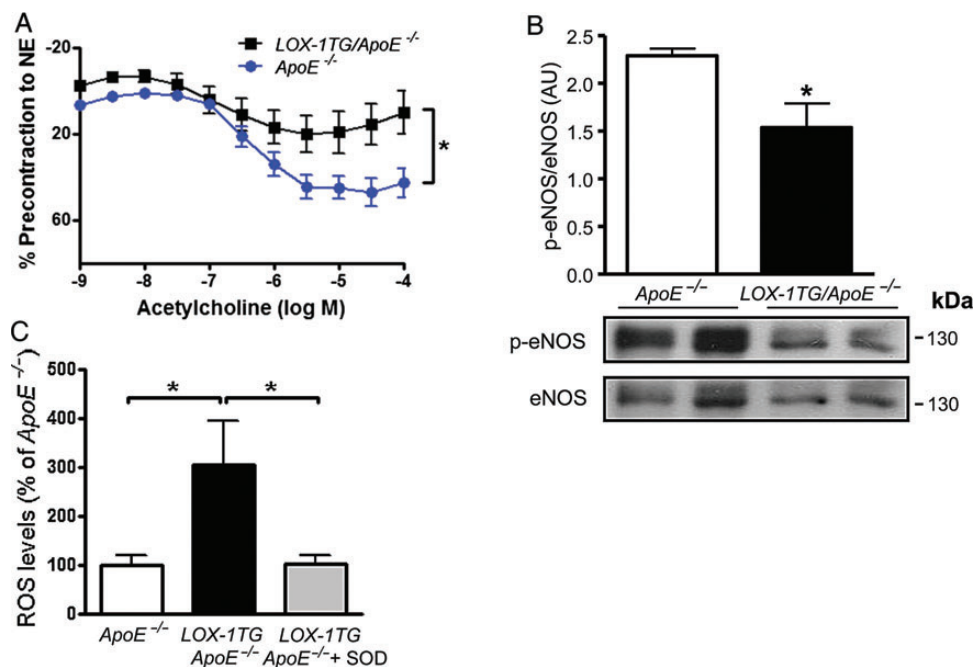
Figure 5 Increased plaque formation is associated with endothelial dysfunction, decreased endothelial nitric oxide synthase phosphorylation and increased ROS levels in *LOX-1TG/ApoE*$^{-/-}$ mice. (A) Relaxation to increasing concentrations of acetylcholine in aortic rings from *ApoE*$^{-/-}$ and *LOX-1TG/ApoE*$^{-/-}$ mice. Values were normalized to preconstruction with U46619 and shown as mean $\pm$ SEM. *ApoE*$^{-/-}$ (blue line), *LOX-1TG/ApoE*$^{-/-}$ (black line). $n = 8$/genotype, *$P < 0.05$. (B) Western blot reveals decreased endothelial nitric oxide synthase activation through phosphorylation of Ser1177 residue in aortic lysates from *LOX-1TG/ApoE*$^{-/-}$ mice. Quantification of protein expression is given as ratio to total endothelial nitric oxide synthase expression levels; $n = 4$ for each group, *$P < 0.05$. Statistical significance was calculated with unpaired Student's *t*-test. (C) Measurements of total reactive oxygen species production by electron spin resonance spectroscopy in aortas show increased reactive oxygen species levels in *LOX-1TG/ApoE*$^{-/-}$ mice compared with *ApoE*$^{-/-}$ controls. Pre-treatment of aortas from *LOX-1TG/ApoE*$^{-/-}$ mice with 150 U/mL SOD significantly reduces reactive oxygen species accumulation. Quantification is given as a percentage of average control value; $n = 6$ for each group, *$P < 0.05$.

dysfunction and accelerates plaque formation; (iii) endothelium-targeted LOX-1 overexpression increases aortic ROS production and activates redox-sensitive pathways such as MAPK p38 and NFκB, ensuing in endothelial inflammation.

Uptake of oxLDL by endothelial cells and macrophages is a key event preceding plaque formation (i) and (ii). However, it is not clear whether endothelial LOX-1 activation translates into an atherolsclerotic phenotype in the vasculature. In the present study, we have demonstrated that endothelial overexpression of LOX-1 accelerates endothelial dysfunction in atherosclerosis-prone *ApoE*$^{-/-}$ mice. This finding is in line with the notion that LOX-1 antagonism improves NO availability in the coronary circulation.[24] Indeed, we have found that in *LOX-1TG* mice LOX-1 overexpression induces oxidative stress and reduces eNOS activation without affecting endothelial function. In contrast, using *LOX-TG1/ApoE*$^{-/-}$ mice, we have observed impaired vasorelaxation to acetylcholine. We do speculate that in *LOX-1TG* mice some compensatory mechanisms may still be operating in the absence of a severe atherosclerotic phenotype. Another possibility is that increased ROS production observed in *LOX-1TG* mice was not sufficient to affect endothelium-dependent relaxation by such a strong agonist as acetylcholine. Impaired vasorelaxation in *LOX-1TG/*

ApoE$^{-/-}$ mice were explained by reduced eNOS expression and activation as well as increased aortic ROS generation. Indeed, eNOS-activating phosphorylation was blunted in *LOX-1TG/ApoE*$^{-/-}$ mice, thus contributing to endothelial dysfunction observed in these mice. Moreover, LOX-1-dependent oxidative stress led to phosphorylation of MAPK p38 and subsequent activation of NFκB signalling. These molecular events were associated with up-regulation of the inflammatory molecules VCAM-1, E- and P-selectin, favouring monocytes recruitment. Moreover, phosphorylation of p38 is a key initiator of the apoptotic process, thus precipitating vascular pathology in vessels with LOX-1 activation.[25,26] This first set of findings strongly suggests that LOX-1 overexpression in the vascular endothelium is key event preceding the atherogenic process. Indeed, *LOX1-TG* mice without *ApoE*$^{-/-}$ background already showed clear signs of vascular inflammation together with an increased oxidative burden. The strength of our work is the *in vivo* characterization of endothelial LOX-1 in an unanticipated transgenic mouse model. The design of this specific transgene allowed us to understand the relevance of endothelial LOX-1, regardless of its role in macrophages. Notably, we could show that selective activation of LOX-1 in the endothelium is sufficient to induce early precursors of atherosclerotic disease such as

endothelial dysfunction and NFκB-driven inflammation. Indeed, macrophages did not show any up-regulation or functional activity of LOX-1 in our genetic model, further strengthening the importance of endothelial LOX-1 in atherogenesis. Although under certain conditions the *Tie2* promoter may also be active in macrophages,[27,28] it appears that other scavenger receptors play a more dominant role for the oxLDL uptake in these cells. Indeed, our initial characterization of the *LOX-1TG* mice revealed high levels of LOX-1 transgene mRNA in aortic endothelial cells, and lower levels in peritoneal macrophages. However, functional assay of oxLDL uptake showed no difference between transgenic and non-transgenic macrophages ruling out a contribution of other scavenger receptors such as SR-A and SR-B under our experimental conditions. Moreover, bone marrow transplantation experiments together with immunostaining of atherosclerotic aortas demonstrated that bone marrow-derived cells, in particular macrophages, do not account for the increase in atherosclerosis observed in our LOX-1 transgenic mouse model. Thus, we were able to specifically overexpress LOX-1 in the endothelium of mice *in vivo* and to demonstrate distinct functional changes of endothelial cells, i.e. a marked increase in oxLDL uptake as a crucial step in the atherosclerosis process.

Since plasma lipid levels were similar in *LOX-1TG* and WT mice, the difference in fatty streak formation observed in transgenic mice must be related to an increased activity of the LOX-1 receptor as demonstrated in transgenic endothelial cells in culture. Indeed, aortic levels of lipoproteins were augmented in *LOX-1TG* as compared with WT littermates. Using a preproendothelin-1 promoter and a bovine *LOX-1* transgene, others found no phenotype of the transgene in WT C57BL/6 mice, but an inflammatory intramyocardial vasculopathy on the *ApoE* background.[7] This discrepancy may be related to the fact that the preproendothelin-1 promoter, unlike the *Tie2* promoter used in our study, drives *LOX-1* transgene expression predominantly in microvessels rather than in conduit arteries that are prone to atherosclerotic plaque formation. Furthermore, species differences between bovine and murine *LOX-1* gene may have contributed.

In summary, our data indicate that endothelial-specific overexpression of LOX-1 enhances lipid deposition and inflammation in the aorta and leads to endothelial dysfunction and atherosclerotic plaque formation. At the molecular level, LOX-1 activates p38-NFκB pathway resulting in increased VCAM-1, E- and P-selectin transcription, and vascular inflammation. As LOX-1 is also overexpressed in human plaques, endothelial-specific inhibition of LOX-1 may represent a new therapeutic target for the prevention and treatment of atherosclerosis.

Study limitations

There are still some limitations applied for the present study which need to be considered and addressed in the future. First of all, extrapolation of data obtained in genetically modified mice to human is always a difficult issue. Therefore, in order to support our conclusion regarding clinical applications, further experiments on human samples should be considered in the future. Second, the use of transgenic mice does not completely exclude the existence of alternative LOX-1-dependent molecular pathways. Finally, smooth muscle cells may also contribute to LOX-1-mediated atherogenesis, since the basal expression of LOX-1 and the activity of *Tie2* promoter have been previously reported in these cells.

Supplementary material

Supplementary material is available at *European Heart Journal* online.

References

1. Witztum JL, Steinberg D. Role of oxidized low density lipoprotein in atherogenesis. *J Clin Invest* 1991;**88**:1785–1792.
2. Zingg JM, Ricciarelli R, Azzi A. Scavenger receptor regulation and atherosclerosis. *Biofactors* 2000;**11**:189–200.
3. Mehta JL, Chen J, Hermonat PL, Romeo F, Novelli G. Lectin-like, oxidized low-density lipoprotein receptor-1 (LOX-1): a critical player in the development of atherosclerosis and related disorders. *Cardiovasc Res* 2006;**69**:36–45.
4. Pluddemann A, Neyen C, Gordon S. Macrophage scavenger receptors and host-derived ligands. *Methods* 2007;**43**:207–217.
5. Chen M, Narumiya S, Masaki T, Sawamura T. Conserved C-terminal residues within the lectin-like domain of LOX-1 are essential for oxidized low-density-lipoprotein binding. *Biochem J* 2001;**355**:289–296.
6. Ross R. Atherosclerosis – an inflammatory disease. *N Engl J Med* 1999;**340**:115–126.
7. Inoue K, Arai Y, Kurihara H, Kita T, Sawamura T. Overexpression of lectin-like oxidized low-density lipoprotein receptor-1 induces intramyocardial vasculopathy in apolipoprotein E-null mice. *Circ Res* 2005;**97**:176–184.
8. Mehta JL, Sanada N, Hu CP, Chen J, Dandapat A, Sugawara F, Satoh H, Inoue K, Kawase Y, Jishage K, Suzuki H, Takeya M, Schnackenberg L, Beger R, Hermonat PL, Thomas M, Sawamura T. Deletion of LOX-1 reduces atherogenesis in LDLR knockout mice fed high cholesterol diet. *Circ Res* 2007;**100**:1634–1642.
9. Kataoka H, Kume N, Miyamoto S, Minami M, Moriwaki H, Murase T, Sawamura T, Masaki T, Hashimoto N, Kita T. Expression of lectinlike oxidized low-density lipoprotein receptor-1 in human atherosclerotic lesions. *Circulation* 1999;**99**:3110–3117.
10. Li D, Mehta JL. Antisense to LOX-1 inhibits oxidized LDL-mediated upregulation of monocyte chemoattractant protein-1 and monocyte adhesion to human coronary artery endothelial cells. *Circulation* 2000;**101**:2889–2895.
11. Li D, Chen H, Romeo F, Sawamura T, Saldeen T, Mehta JL. Statins modulate oxidized low-density lipoprotein-mediated adhesion molecule expression in human coronary artery endothelial cells: role of LOX-1. *J Pharmacol Exp Ther* 2002;**302**:601–605.
12. Cominacini L, Rigoni A, Pasini AF, Garbin U, Davoli A, Campagnola M, Pastorino AM, Lo Cascio V, Sawamura T. The binding of oxidized low density lipoprotein (ox-LDL) to ox-LDL receptor-1 reduces the intracellular concentration of nitric oxide in endothelial cells through an increased production of superoxide. *J Biol Chem* 2001;**276**:13750–13755.
13. Becher B, Durell BG, Miga AV, Hickey WF, Noelle RJ. The clinical course of experimental autoimmune encephalomyelitis and inflammation is controlled by the expression of CD40 within the central nervous system. *J Exp Med* 2001;**193**:967–974.
14. von Lukowicz T, Hassa PO, Lohmann C, Boren J, Braunersreuther V, Mach F, Odermatt B, Gersbach M, Camici GG, Stahli BE, Tanner FC, Hottiger MO, Luscher TF, Matter CM. PARP1 is required for adhesion molecule expression in atherogenesis. *Cardiovasc Res* 2008;**78**:158–166.
15. Kobayashi M, Inoue K, Warabi E, Minami T, Kodama T. A simple method of isolating mouse aortic endothelial cells. *J Atheroscler Thromb* 2005;**12**:138–142.
16. Biocca S, Falconi M, Filesi I, Baldini F, Vecchione L, Mango R, Romeo F, Federici G, Desideri A, Novelli G. Functional analysis and molecular dynamics simulation of LOX-1 K167N polymorphism reveal alteration of receptor activity. *PLoS ONE* 2009;**4**:e4648.
17. Madonna R, Salerni S, Schiavone D, Glatz JF, Geng YJ, De Caterina R. Omega-3 fatty acids attenuate constitutive and insulin-induced CD36 expression through a suppression of PPAR alpha/gamma activity in microvascular endothelial cells. *Thromb Haemost* 2011;**106**:500–510.

18. Plump AS, Smith JD, Hayek T, Aalto-Setala K, Walsh A, Verstuyft JG, Rubin EM, Breslow JL. Severe hypercholesterolemia and atherosclerosis in apolipoprotein E-deficient mice created by homologous recombination in ES cells. *Cell* 1992;**71**:343–353.

19. Imanishi T, Hano T, Sawamura T, Takarada S, Nishio I. Oxidized low density lipoprotein potentiation of Fas-induced apoptosis through lectin-like oxidized-low density lipoprotein receptor-1 in human umbilical vascular endothelial cells. *Circ J* 2002;**66**: 1060–1064.

20. Chen J, Mehta JL, Haider N, Zhang X, Narula J, Li D. Role of caspases in Ox-LDL-induced apoptotic cascade in human coronary artery endothelial cells. *Circ Res* 2004;**94**:370–376.

21. Li D, Liu L, Chen H, Sawamura T, Ranganathan S, Mehta JL. LOX-1 mediates oxidized low-density lipoprotein-induced expression of matrix metalloproteinases in human coronary artery endothelial cells. *Circulation* 2003;**107**:612–617.

22. Mehta JL, Chen J, Yu F, Li DY. Aspirin inhibits ox-LDL-mediated LOX-1 expression and metalloproteinase-1 in human coronary endothelial cells. *Cardiovasc Res* 2004; **64**:243–249.

23. Weber C, Erl W, Pietsch A, Strobel M, Ziegler-Heitbrock HW, Weber PC. Antioxidants inhibit monocyte adhesion by suppressing nuclear factor-kappa B mobilization and induction of vascular cell adhesion molecule-1 in endothelial cells stimulated to generate radicals. *Arterioscler Thromb* 1994;**14**:1665–1673.

24. Xu X, Gao X, Potter BJ, Cao JM, Zhang C. Anti-LOX-1 rescues endothelial function in coronary arterioles in atherosclerotic ApoE knockout mice. *Arterioscler Thromb Vasc Biol* 2007;**27**:871–877.

25. Bao MH, Zhang YW, Zhou HH. Paeonol suppresses oxidized low-density lipoprotein induced endothelial cell apoptosis via activation of LOX-1/p38MAPK/ NF-kappaB pathway. *J Ethnopharmacol* 2013;**146**:543–551.

26. Ogura S, Kakino A, Sato Y, Fujita Y, Iwamoto S, Otsui K, Yoshimoto R, Sawamura T. Lox-1: the multifunctional receptor underlying cardiovascular dysfunction. *Circ J* 2009;**73**:1993–1999.

27. De Palma M, Venneri MA, Galli R, Sergi Sergi L, Politi LS, Sampaolesi M, Naldini L. Tie2 identifies a hematopoietic lineage of proangiogenic monocytes required for tumor vessel formation and a mesenchymal population of pericyte progenitors. *Cancer Cell* 2005;**8**:211–226.

28. De Palma M, Venneri MA, Roca C, Naldini L. Targeting exogenous genes to tumor angiogenesis by transplantation of genetically modified hematopoietic stem cells. *Nat Med* 2003;**9**:789–795.

CARDIOVASCULAR FLASHLIGHT

Surgical banding of the inferior vena cava for the facilitation of transcatheter valve implantation in a patient with severe secondary tricuspid regurgitation

Georg Daniel Duerr[1*†], **Matthias Endlich**[1†], **Jan-Malte Sinning**[2], **Bahman Esmailzadeh**[1], **Nikos Werner**[2], and **Fritz Mellert**[1]

[1]Department of Cardiac Surgery, University Clinical Center of Bonn, Bonn, Germany; and [2]Department of Cardiology, Pneumology and Angiology, Medizinische Klinik II, University Clinical Center of Bonn, Bonn, Germany

* Corresponding author. E-mail: daniel.duerr@ukb.uni-bonn.de
† These authors contributed equally to this work.

Pathological tricuspid regurgitation (TR) is more often secondary due to annular dilatation and increased tricuspid leaflet tethering. Although ring annuloplasty is key to surgery for TR, surgical treatment of TR in high-risk patients is associated with increased mortality. Percutaneous single or dual caval transcatheter heart valve-(THV)-prosthesis implantation seems feasible, but not realizable in many patients due to increased caval vein diameter.

In an 85-year-old woman with severe TR (*Panels A and B*) associated with advanced right-heart failure, ascites, and portal hypertension (*Panel C*) at prohibitive risk for open-heart surgery (EuroSCORE 21.7), transesophageal echocardiography (TEE) and multi-slice computed tomography (MSCT) revealed inferior vena cava (IVC) dilatation (*Panel D*; 34 × 43 mm).

To downsize the IVC to a mean diameter <30 mm, surgical banding was performed via right-lateral mini-thoracotomy using a longitudinally-opened goretex-prosthesis, which was 'wrapped' around the IVC below the diaphragm just after the confluence of the hepatic veins, while a 30 mm Z-MED II valvuloplasty balloon was inflated in that position. Thereafter, a balloon-expandable

stent (AndraStent-XXL, 35 mm, Andramed) was deployed within the banded IVC-segment, which was tightened with 5-0 Prolene-suture. Finally, an Edwards-SAPIEN 29 mm was implanted into the stent (*Panels E and F*).

Although pacemaker leads in the superior vena cava (SVC) prohibited implantation of an upper caval valve, TR declined significantly (*Panels G–I*), and general condition had significantly improved at discharge after 2 weeks (decreased ascites and peripheral oedema; 9 kg weight loss). TEE/MSCT showed trace-leakage with decrease of RV and RA volumes and hepatic vein diameters.

We conclude that in high-risk patients with severe TR and enlarged IVC, downsizing of IVC is feasible to enable THV implantation.